Natural Occurrence of Autoantibodies against Basement Membrane Proteins in Epidermolysis Bullosa

Gostyński, Antoni; Diercks, Gilles F H; Escamez, Maria-José; Chandran, Nisha Suyien; de Lucas, Raúl; Garcia-Martin, Adela; Del Rio, Marcela; Bremer, Jeroen; Bolling, Maria C; Meana, Alvaro

Published in:
Journal of Investigative Dermatology

DOI:
10.1016/j.jid.2021.10.030

Publication date:
2022

Human Molecular Genetics, 2022, Vol. 00, 00, 1–14
https://doi.org/10.1093/hmg/ddac053
Advance access publication date: 2 March 2022
Original Article

De novo variants in *EMC1* lead to neurodevelopmental delay and cerebellar degeneration and affect glial function in *Drosophila*

Hyung-Lok Chung[1,2,3], Patrick Rump[4], Di Lu[1,2], Megan R. Glassford[5], Jung-Wan Mok[1,2], Jawid Fatih[1], Adily Basal[6], Paul C. Marcogliese[1,2], Oguz Kanca[1,2], Michele Rapp[7], Johanna M. Fock[8], Erik-Jan Kamsteeg[9], James R. Lupski[1,10,11], Austin Larson[12], Mark C. Haninbal[5], Hugo Bellen[1,2,3,*] and Tamar Harel[6,13,*]

[1]Department of Molecular and Human Genetics, Baylor College of Medicine, Houston, TX 77030, USA
[2]Jan and Dan Duncan Neurological Research Institute, Texas Children's Hospital, Houston, TX 77030, USA
[3]Howard Hughes Medical Institute, Baylor College of Medicine, Houston, TX 77030, USA
[4]University of Groningen, University Medical Centre Groningen, Department of Genetics, Groningen 9700 RB, The Netherlands
[5]Division of Pediatric Genetics, Metabolism & Genomic Medicine, University of Michigan Medical School, Ann Arbor, MI 48109, USA
[6]Department of Genetics, Hadassah Medical Organization, Jerusalem 9112001, Israel
[7]University of Colorado Anschutz Medical Campus, Aurora, CO 60045, USA
[8]University of Groningen, University Medical Centre Groningen, Department of Neurology, Groningen 9700 RB, The Netherlands
[9]Department of Human Genetics, Radboud University Medical Centre, Nijmegen 6500 HB, The Netherlands
[10]Human Genome Sequencing Center, Baylor College of Medicine, Houston, TX 77030, USA
[11]Department of Pediatrics, Texas Children's Hospital, Houston, TX 77030, USA
[12]University of Colorado School of Medicine and Children's Hospital Colorado, Aurora, CO 60045, United States
[13]Faculty of Medicine, Hebrew University of Jerusalem, Jerusalem 9112001, Israel
*To whom correspondence should be addressed at: Department of Genetics, Hadassah-Hebrew University Medical Center, POB 12000, Jerusalem 9112001, Israel. Tel: +(972)-2-6776329; Fax: +(972)-2-6777618; Email: tamarhe@hadassah.org.il; Department of Molecular and Human Genetics, Baylor College of Medicine, Houston, TX 77030, USA. Tel: +1 832824-8750; Fax: +1832825-1240; Email: hbellen@bcm.edu

Abstract

Background: The endoplasmic reticulum (ER)-membrane protein complex (EMC) is a multi-protein transmembrane complex composed of 10 subunits that functions as a membrane-protein chaperone. Variants in *EMC1* lead to neurodevelopmental delay and cerebellar degeneration. Multiple families with biallelic variants have been published, yet to date, only a single report of a monoallelic variant has been described, and functional evidence is sparse.
Methods: Exome sequencing was used to investigate the genetic cause underlying severe developmental delay in three unrelated children. *EMC1* variants were modeled in *Drosophila*, using loss-of-function (LoF) and overexpression studies. Glial-specific and neuronal-specific assays were used to determine whether the dysfunction was specific to one cell type.
Results: Exome sequencing identified de novo variants in *EMC1* in three individuals affected by global developmental delay, hypotonia, seizures, visual impairment and cerebellar atrophy. All variants were located at Pro582 or Pro584. *Drosophila* studies indicated that imbalance of *EMC1*—either overexpression or knockdown—results in pupal lethality and suggest that the tested homologous variants are LoF alleles. In addition, glia-specific gene dosage, overexpression or knockdown, of *EMC1* led to lethality, whereas neuron-specific alterations were tolerated.
Discussion: We establish de novo monoallelic *EMC1* variants as causative of a neurological disease trait by providing functional evidence in a *Drosophila* model. The identified variants failed to rescue the lethality of a null allele. Variations in dosage of the wild-type *EMC1*, specifically in glia, lead to pupal lethality, which we hypothesize results from the altered stoichiometry of the multi-subunit protein complex EMC.

Introduction

The endoplasmic reticulum (ER) membrane protein complex (EMC) is a multi-protein transmembrane complex composed of 10 subunits, EMC1–EMC10 (1). EMC binds to the ER-associated degradation machinery and functions as a membrane protein chaperone for a subset of tail-anchored (TA) proteins and many multi-pass integral transmembrane proteins (2,3). The role of EMC has been reported in a diverse set of cellular processes such as protein quality control, biosynthesis of membrane proteins and phospholipids, and virus replication (1,4).

Pathogenic variants in *EMC1* [MIM 616846] and *EMC10* [MIM 614545], encoding two of the EMC subunits, have been associated with human disease. *EMC1* variants have been implicated in cerebellar atrophy, visual impairment and psychomotor retardation [MIM 616875]. Biallelic variants have been identified in five families with a neurological phenotype and a single family with non-syndromic retinitis pigmentosa, whereas monoallelic variants have been reported in a single patient with a neurological phenotype and in association with cardiac malformations (5–10).

Received: August 20, 2021. **Revised:** February 22, 2022. **Accepted:** February 23, 2022

Studies in *Xenopus tropicalis* revealed a critical role for *emc1* in neural crest development and Wnt signaling, with mislocalization of transmembrane proteins upon *emc1* depletion. Modeling of *EMC1* variants, reported in humans as likely pathogenic for diverse phenotypes, suggested that these were mostly loss-of-function (LoF) alleles in *Xenopus* (11). Recently, homozygous *EMC10* variants were described in individuals with a neurodevelopmental disorder with dysmorphic facies and variable seizures (NEDDFAS, MIM 619264) (12,13), partially overlapping with *EMC1*-associated disease.

In this study, we report three de novo *EMC1* variants in sporadic probands and provide evidence for rare variant pathogenicity in a *Drosophila* model. Furthermore, we demonstrate that EMC1 is required for proper glial function.

Results

De novo variants in three affected individuals localize to a specific region of EMC1

Detailed clinical case descriptions are provided in Supplemental Data and summarized in Table 1. The three unrelated children (Fig. 1A and Supplementary Material, Figs S1–S5) described all had severe to profound developmental delay, truncal hypotonia, seizures and cortical visual impairment. Two children (Families A and B) had increased tone in the extremities, diminished deep tendon reflexes and dystonic posturing. No specific craniofacial pattern of dysmorphic features or gestalt was recognized. Brain MRIs in Families A and C showed cerebellar atrophy/hypoplasia, whereas the proband in Family B seemed to have a normal cerebellum at 13 years of age, necessitating further follow-up. Overall, the phenotypic features were consistent with previous reports (Table 1). Hip dysplasia (Families A and C) and neurogenic bowel and bladder (Family B) phenotypes were phenotypic expansions to the trait described thus far as they are not previously reported within the *EMC1*-associated clinical spectrum.

A likely pathogenic variant in *EMC1* was identified in each of the three probands. In Family A, a de novo variant (chr1:19559155G > T[hg19]; NM_015047.3: c.1745C > A; p.(Pro582His)) was identified and confirmed by Sanger sequencing (Supplementary Material, Figs S2 and S3) by trio exome sequencing. In Family B, exome sequencing of the proband and his mother was carried out; the father had died in a motor vehicle accident during the pregnancy and DNA was not available. Exome sequencing revealed a heterozygous *EMC1* variant in the proband but not in his mother: chr1:19559155G > C[hg19]; NM_015047.3: c.1745C > G; p.(Pro582Arg). A second variant was not identified, and copy number analysis from exome read depth was normal. The variant read count was 11 of 87 reads (12.6%), suggesting post-zygotic mosaicism and de novo occurrence of the c.1745C > G variant in the child. The variant was confirmed by Sanger sequencing (Supplementary Material, Fig. S5). In Family C, trio exome sequencing revealed a de novo variant in *EMC1*: chr1:19559149G > T[hg19]; NM_015047.3: c.1751C > A; p.(Pro584His), confirmed by Sanger sequencing (Supplementary Material, Fig. S6). Thus, all three are predicted by conceptual translation to represent missense alleles.

The three de novo variants all affect either Pro582 or Pro584 (Fig. 1B and C), and no second *EMC1* variant was identified in these patients, with the caveat that only exome sequencing rather than whole genome sequencing was available for all probands. To further address this, we amplified and sequenced the full coding sequence of *EMC1* cDNAs derived from fibroblasts of Individual II1 of Family A. We did not observe any mis-splicing events, and observed representation of both the wild-type and mutant copies of the *EMC1* variant (Supplementary Material, Fig. S3). This suggests that there were no deep intronic or regulatory variants significantly affecting the second copy of the gene. No other pathogenic or likely pathogenic variants in other genes were identified in the affected children. Taken together, these data suggest that alterations of these specific residues are pathogenic and may be dominant. According to American College of Medical Genetics and Genomics (ACMG) guidelines, the variants were all classified as pathogenic or likely pathogenic (Supplementary Material, Table S1).

ClinVar (https://www.ncbi.nlm.nih.gov/clinvar) lists a c.1754C > A; p.(Pro585Gln) variant as likely pathogenic, in a patient with cerebellar atrophy, visual impairment and psychomotor retardation (accession number VCV000801454.1), potentially supporting our observation of a critical residue; albeit, no data are provided regarding zygosity and inheritance of the variant. However, gnomAD (https://gnomad.broadinstitute.org/) (14) lists adjacent variants in individuals unaffected by a severe childhood syndrome: p.(His583Arg) in two individuals and p.(Pro584Thr) in a third individual. The proximity of several pathogenic/likely pathogenic variants and purported benign variants within a range of three amino acids, some affecting the identical residue, warrants cautious variant interpretation and functional biology investigations of these rare variants in a model organism.

In silico analysis of protein structure

The Cryo-EM structure of the human EMC (PDB ID: 7ADO) (15) showed that the affected residues are located in a loop connecting two β-strands in an eight-bladed β-propeller structure of EMC1. They are in close proximity to residue Gly471, previously identified as a de novo variant in *EMC1* (7) (Fig. 1D). β-propellers commonly use a proline at the boundary between the loop and the β-strand, to disfavor further β interactions by providing both a very strong local twist and also a local outward protrusion (16), because of the cyclic structure of the proline. Thus, substitutions at the prolines may

Table 1. Clinical features of patients with *EMC1* variants and neurological phenotypes

	Biallelic variants							Monoallelic variants			
Family	**Harel *et al.*, 2016: Family 1**	**Harel *et al.*, 2016: Family 2**			**Harel *et al.*, 2016: Family 3**		**Geetha *et al.*, 2018**	**Cabet *et al.*, 2020**	**Harel *et al.*, 2016: Family 4**	**Current report: Family A**	**Current report: Family B**	**Current report: Family C**
Individual	A3	BAB3445	BAB3446	BAB3447	BAB6896	BAB6897			BH4387_1			
Age at last exam	4 yr	13 yr	5 yr	3 yr	10 yr	12 yr	4 yr, 10 mo	10 yr	11 yr	4 yr	15 yr	5 yr
Global developmental delay	Yes	Yes	Yes	Yes	Yes	Yes	Yes, severe		Yes	Yes, profound	Yes, profound	Yes, severe
Speech delay	Yes	Yes	Yes	Yes	Yes	Yes	No speech	No speech	Yes	No speech	No speech	No speech
Seizures	Yes, subclinical	No	No	No	No	No	Early infantile, myoclonic jerks and generalized tonic–clonic	No	No	Early onset, refractory, absences, tonic, clonic and tonic–clonic seizures, myoclonia	Absence	Yes
Scoliosis	Yes	Yes	Yes	Yes	Yes	No	Yes	No	Yes	Yes	Yes	No
Postnatal microcephaly	3–10%ile (2 yr 9mo)	Yes	Yes	Yes	No	No	Yes	No	6th %ile (18mo)	No (−0.76 sd); yet exhibited a postnatal decline in percentiles	Yes	No
Dysmorphic features	Short upper lip, mild hypertelorism, retrognathia	Deep set eyes, gingival hyperplasia, short philtrum, retrognathia, persistent fetal finger pads	Deep set eyes, gingival hyperplasia, short philtrum, retrognathia, persistent fetal finger pads	Deep set eyes, gingival hyperplasia, short philtrum, retrognathia, persistent fetal finger pads	Deep set eyes, retrognathia	Deep set eyes		No	Dysplastic ears	Scapho-cephaly	No	No
Truncal hypotonia	Yes	Yes	Yes	Yes	Yes	No	Yes	Yes	Yes	Yes	Yes	Yes
Increased tone in extremities	Yes	Yes	Yes	Yes	No	No		No	No	Yes	Yes	No
Diminished DTRs	Yes	Yes	Yes	Yes	Na	No	Yes	No	Yes	Yes	Yes	Yes in upper extremities, brisk reflexes in lower extremities

Continued

Table 1. Continued

	Biallelic variants								Monoallelic variants			
Family	**Harel *et al.*, 2016: Family 1**	**Harel *et al.*, 2016: Family 2**			**Harel *et al.*, 2016: Family 3**		**Geetha *et al.*, 2018**	**Cabet *et al.*, 2020**	**Harel *et al.*, 2016: Family 4**	**Current report: Family A**	**Current report: Family B**	**Current report: Family C**
Dystonic posturing	Yes	Yes	Yes	Yes	No	No	Yes	No	No	Yes	Yes	No
Abnormal ophthalmology exam	Cortical visual impairment	Abnormal VEP and erg	Abnormal VEP and erg	Abnormal VEP and erg	Esotropia, hyperopia, astigmatism	Na	Visual impairment	Intermittent unilateral divergent strabismus, possible amblyopia	Myopia, optic atrophy	Cortical visual impairment; no response on VEP	Cortical visual impairment, hyperopia	Cortical visual impairment, roving eye movement
Cerebellar atrophy or hypoplasia	Yes	Yes	Yes	Yes	Yes	Na	Yes, severe	No	Yes	Yes, progressive	No	Yes, mild
Other brain MRI findings	Cerebral atrophy, cc atrophy, small hippocampi	Cerebral atrophy, thin and foreshortened cc	Cerebral atrophy, thin and foreshortened cc	Cerebral atrophy, thin and foreshortened cc	Foreshortened cc	Na	Mild diffuse atrophy in supratentorial compartment		Mild cerebral atrophy, foreshortened cc	Thin cc	Bilateral foci of increased white matter signal - subcortical, periventricular, and along cerebellum; cerebral atrophy, thin splenium of cc	No
Other clinical findings	Laryngotracheomalacia, imperforate anus						Scaphocephaly, deep-set eyes	Autism spectrum disorder, plagiocephaly, bifid uvula		Feeding difficulties; hip dysplasia; pectus carinatum	Symmetric growth delay; neurogenic bladder and bowel; osa and hypoventilation; contracture of right hand	Hip dysplasia, sialorrhea, behavioral difficulties (biting self, screaming)
Variants in *EMC1* (NM_015047.3)	c.2619_2622delTCCT; p.Pro874Argfs*21 (hom)	c.245C > T;p.Thr82Met (hom)	c.245C > T;p.Thr82Met (hom)	c.245C > T;p.Thr82Met (hom)	c.2602G > A; p.Gly868Arg (hom)	c.2602G > A; p.Gly868Arg (hom)	c.1212 + 1G > A (hom)	c.1134C > A; p.Tyr378Ter; c.2858 T > C; p.Phe953Ser (comp het)	c.1411G > C; p.Gly471Arg (de novo)	c.1745C > A; p.Pro582His (de novo)	c.1745C > G; p.Pro582Arg (mosaic; not inherited from mother, father deceased)	c.1751C > A; p.Pro584His (de novo)

CC—corpus callosum, DTR—deep tendon reflexes, EEG—electroencephalogram, ERG—electroretinogram, NA—not available, OSA—obstructive sleep apnea, VEP—visual evoked potential.

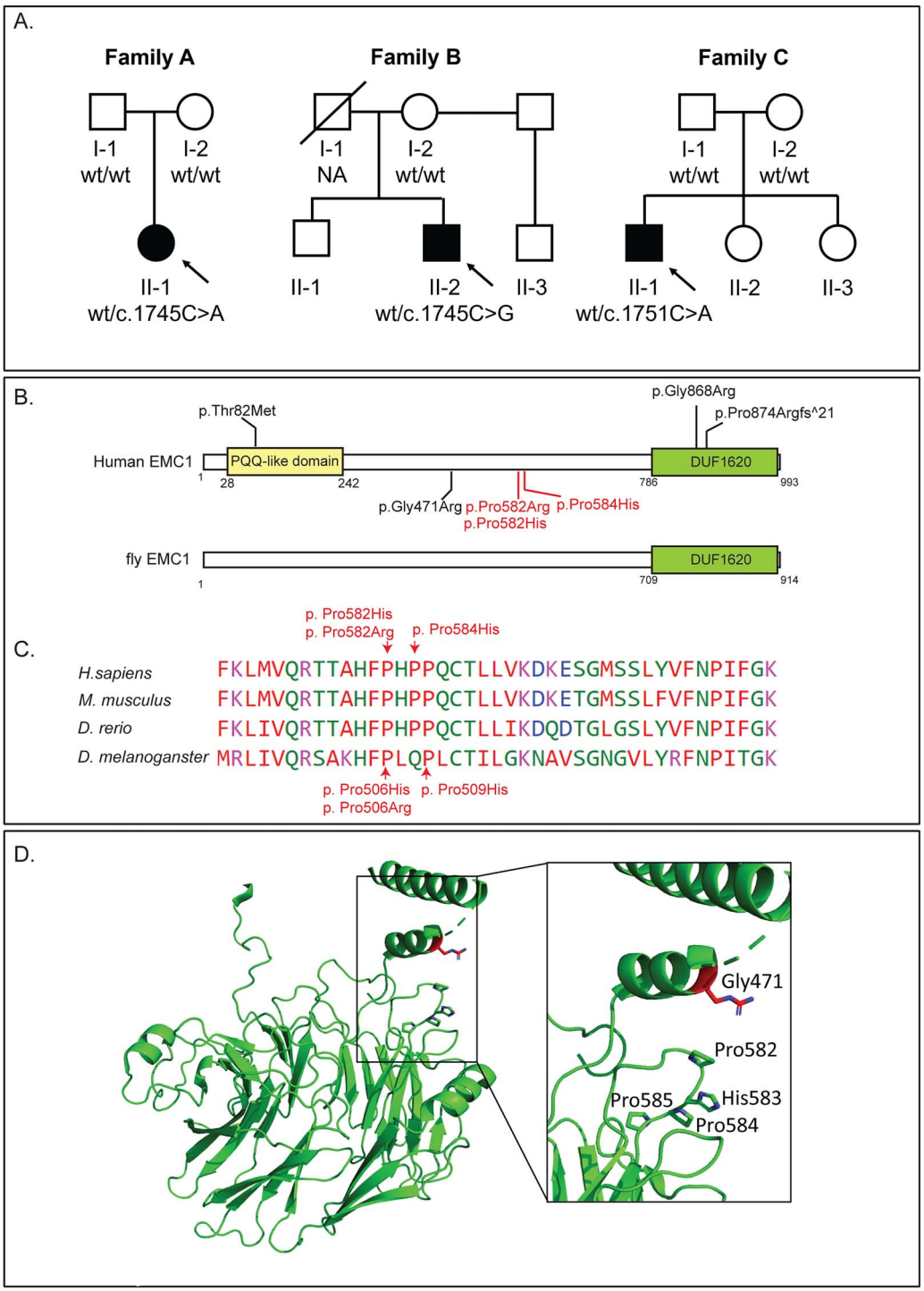

Figure 1. Pedigree, EMC1 conservation and *in silico* protein modelling. (**A**) Pedigrees of the studied families. (**B**) The domain that includes the variants is highly conserved from fly to human. Biallelic variants are depicted above the protein diagram, and monoallelic variants are shown below the protein diagram. Variants reported here are shown in red. (**C**) Protein sequence alignment in multiple species confirms evolutionary conservation of Pro582 in Drosophila. (**D**) The β-propeller domain of the EMC1 of the Cryo-EM human ER membrane protein complex structure (PDB ID: 7ADO) is shown. The loop region is magnified and shown in the rectangular area, with the known mutated residues in the de novo cases labeled. Pro585 sits at the edge of the loop before the beginning of the β-strand.

disrupt the local conformation of the loop and the interaction between the two β-strands. An alternative plausible hypothesis is that changes in the exposed loop may alter or hinder potential associations with other proteins such as luminal cofactors, as β-propellers are known to function in protein–protein interactions.

Overexpression of wild-type and mutant EMC1 transcripts is toxic in flies

The sole homolog of *EMC1* in the fly is *EMC1* (17). The fly EMC1 and human EMC1 share 48% similarity and 33% identity (18). Human EMC1 includes two conserved domains: a quinoprotein alcohol dehydrogenase-like

domain (PQQ_2) and an as-yet-uncharacterized domain of unknown function 1620 (DUF1620). However, the fly protein only contains the highly conserved DUF1620 domain (Fig. 1B). Protein alignment indicates that the protein domain where the new variants are localized (p. Pro582Arg, p. Pro582His, and p. Pro584His), is mainly conserved across species (Fig. 1C). However, Pro584 specifically is not conserved and is a glutamine residue (Q508) in flies; we therefore reanalyzed this domain on the basis of the structural characteristics of amino acids using Clustal OmegA (19) to predict the functional homolog of p.Pro584 in fly EMC1. The analysis indicates that the domain has a highly conserved structure including hydrophobic (Red)/hydroxyl + Sulfhydryl (Green)/Basic (Magenta) amino acids, and Pro509 in flies seems to functionally replace Pro584 in Human EMC1 (Fig. 1C, see color code). Therefore, we selected the fly *EMC1* p.Pro509His as the homologous mutation of human *EMC1* p.Pro584His.

To test the pathogenicity of the human *EMC1* variants, we generated transgenic flies harboring the homolog fly *EMC1* mutations (Fig. 2A, fly EMC1 p. Pro506Arg, p. Pro506His, and p.Pro509His, respectively) and examined functional differences between the reference gene and variants. We first ubiquitously overexpressed the fly *EMC1* cDNAs using a ubiquitous driver, *Daughterless Gal4* (*Da-Gal4*), in a wild-type background at 25°C. Expression of the wild-type fly *EMC1* cDNA causes pupal lethality (Fig. 2A), suggesting that excess fly EMC1 is toxic. However, the variant cDNAs, when ubiquitously expressed, increase viability to 21% (*EMC1* p.Pro506His), 36% (*EMC1* p.Pro506Arg) and 57% (*EMC1* p. Pro509His), indicating that the variants are less toxic in flies when overexpressed.

P506H, P506R and P509H variants fail to rescue pupal lethality

Homozygotes of the $EMC1^{655G}$ null allele are pupal lethal (20). We confirmed that ubiquitous overexpression of a wild-type fly *EMC1* cDNA could partially rescue the pupal lethality (25%, Fig. 2B) at 25°C. In contrast, all the variants failed to rescue lethality. Hence, the variants function differently *in vivo* compared with the wild-type, and our data support the contention that these variants are LoF mutations (Fig. 2B).

EMC1 is expressed in both glia and neurons

To assess the expression pattern of EMC1 in the nervous system, we generated *EMC1* Kozak GAL4 transgenic flies by using CRISPR-Cas9-mediated homologous recombination approach (21,22). This replaced the coding sequence of the *EMC1* gene with a Kozak consensus-GAL4 gene-dominant marker (Fig. 2C). Two guide RNAs targeting the 5′ and 3′ end of the coding sequence of the gene were used to remove the coding sequence in the presence of a homology donor plasmid with a left and right homology arm. The Kozak sequence followed by the GAL4 gene and a dominant marker (3XP3EGFP) was integrated via homology-directed repair (21,22). Next, we crossed these flies to *UAS-nls mCherry* transgenic flies and co-stained the larval and adult central nervous system (CNS) with a pan-glial marker, anti-Repo and a pan-neuronal marker, anti-elav. The co-staining data indicate that EMC1 is expressed in glia (Fig. 2D) and in neurons.

Loss or gain of *EMC1* in glia is lethal in flies

To investigate which tissue requires EMC1 in the nervous system, we used two independent RNAi transgenes (EMC1 RNAi-1 and EMC1 RNAi-2). We first expressed them ubiquitously to test if a ubiquitous knockdown of EMC1 can mimic the loss of function phenotype and observed pupal lethality as seen in the $EMC1^{655G}$ null allele (Fig. 2B). To validate the efficiency of these EMC1 RNAis, we used *hs-Gal4* (23) crossed with both RNAis and induced heat-shock for an hour in Day 1 males (MATERIALS AND METHODS). We found that the levels of EMC1 transcripts were decreased by 50% (RNAi-1) and 65% (RNAi-2) (Fig. 3A).

EMC1 is known to be expressed in neurons and glia in flies and vertebrates (24,25). Given that most patients carrying *EMC1* variants have several neurodevelopmental phenotypes, we next examined if fly *EMC1* is required in the nervous system. We knocked down *EMC1* in neurons with the *elav-Gal4* driver and the *nsyb-Gal4* driver at 25°C. However, neuronal knockdown of *EMC1* does not cause obvious lethality (Fig. 3B) or other obvious neurobehavioral defects. To increase the efficiency of EMC1 RNAi, we co-expressed the *UAS-Dcr2* and *EMC1 RNAi-1* with *elav-Gal4*. We still did not observed lethality or neurobehavioral defects (data not shown). Next, we tested whether the pan-glial expression of *EMC1 RNAi-1* and 2 by *repo-Gal4* can induce any phenotypes. Indeed, glial knockdown of *EMC1* using *repo-gal4* causes pupal lethality. About 15% of flies eclose, and these escapers exhibit a motor deficit at Day 7 and are very short-lived (~15 days). Notably, co-expression of the human reference *EMC1* nearly fully rescued the pupal lethality (~75–80%) and climbing defects at Day 7 (Fig. 3C), suggesting that both fly *EMC1* and human *EMC1* share conserved functions.

To assess if the glial overexpression of the fly wild-type *EMC1* is toxic or not, we overexpressed the wild-type fly *EMC1* cDNA using *repo-Gal4* at 25°C. Similar to what we observed in glial knockdown experiments, glial overexpression of fly *EMC1* also causes pupal lethality (~4% of flies eclose), whereas the viability was significantly increased (33%, 45% and 62%, respectively) when fly *EMC1* variants were overexpressed in glia (Fig. 3D). In contrast, neuronal overexpression of either reference or fly *EMC1* variants did not cause lethality or neurobehavioral defects (Fig. 3E). These data indicate that glia cells are very susceptible to either loss or gain of fly *EMC* and suggest that the *EMC1* variants found in the three affected individuals have partially lost their function in the three affected individuals.

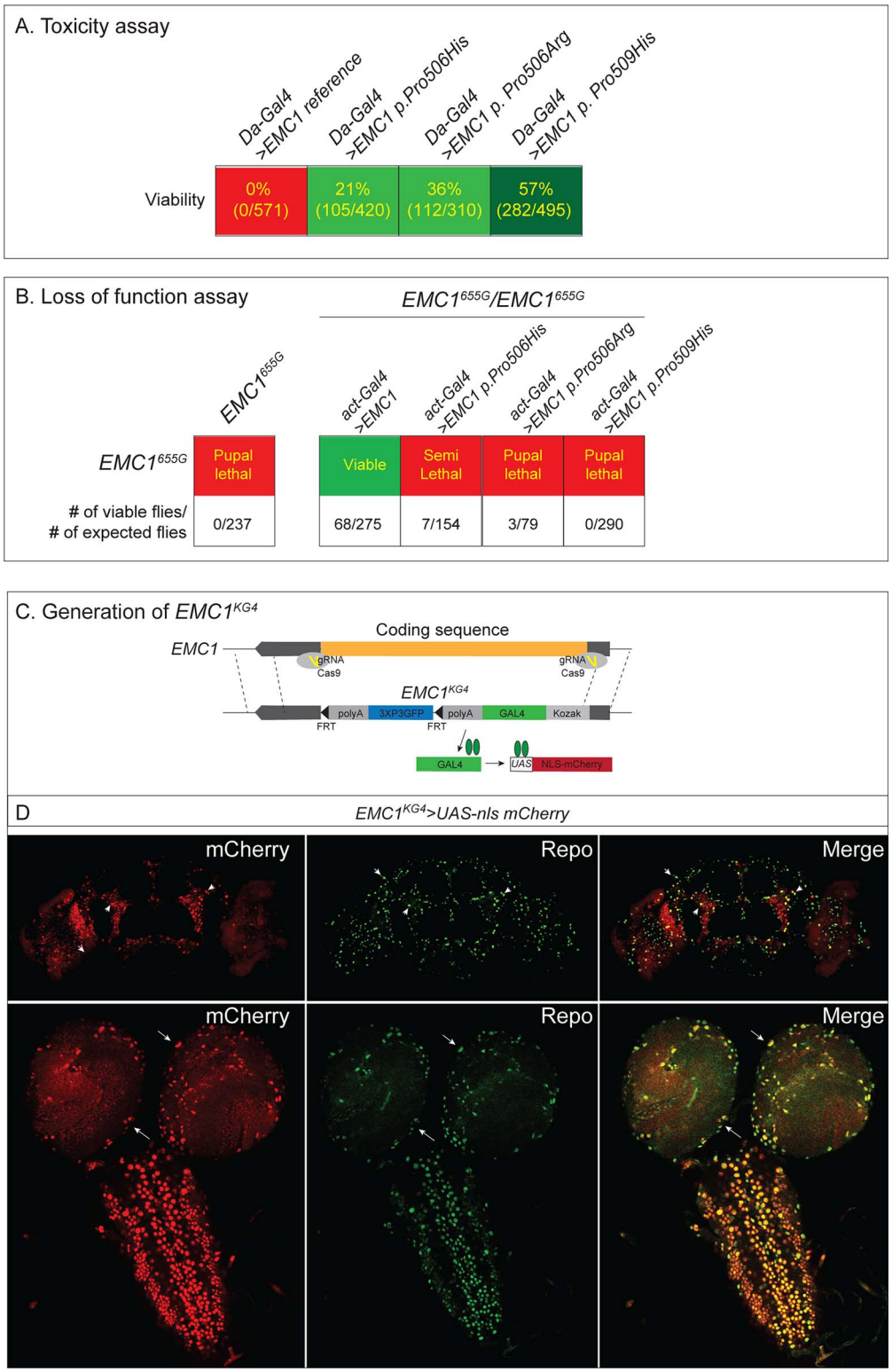

Figure 2. *EMC1* is a functional fly homolog of human *EMC1*. (**A**) Ubiquitous expression of *EMC1* reference using the *Da-GAL4* driver is toxic, but expression of the variants is less toxic. Numbers indicate the ratio of o/e flies. (**B**) Strong ubiquitous expression of *EMC1* reference with *act-GAL4* rescued the pupal lethality observed in $EMC1^{655G}/EMC1^{655G}$ flies, whereas expression of *EMC1 p.Pro506His* or *EMC1 p.Pro509His* variants failed to rescue pupal lethality. Note that the expression of *EMC1 p.Pro506His* results in a few escapers, suggesting that *EMC1 p. Pro506His* is less pathogenic than *EMC1 p.Pro509His* in flies. Numbers indicate the ratio of o/e flies. (**C**) Schematic image showing the locus of $EMC1^{KG4}$ allele. (**D**) An expression pattern of EMC1 in adult CNS (Top) or larval CNS (Bottom). The data suggest that EMC1 is expressed in both neurons and glia.

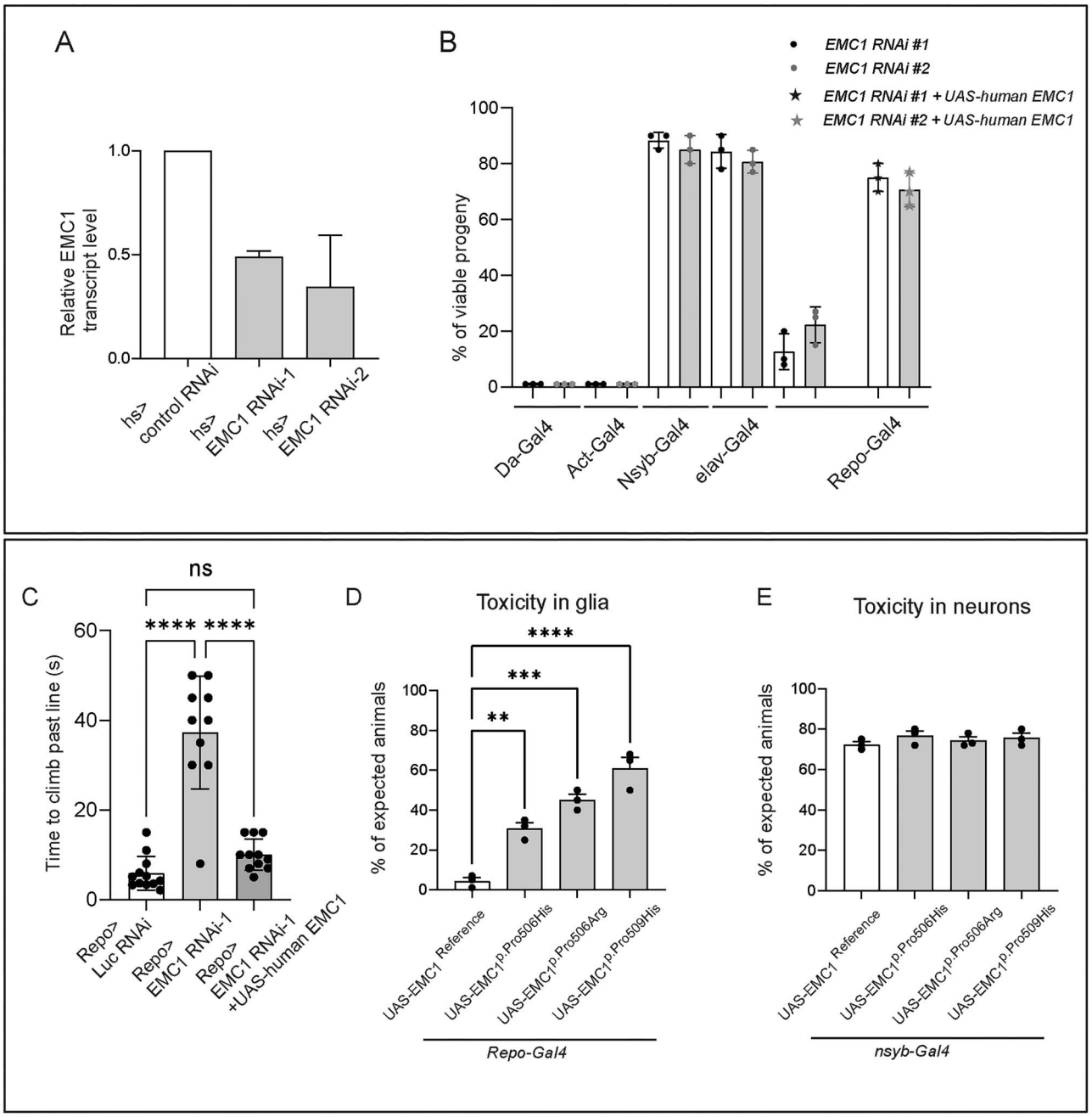

Figure 3. Loss or gain of *EMC1* in glia results in lethality. (**A**) Expression of *EMC1 RNAi-1* or *RNAi-2* by *hs-Gal4* after 1 h heat-shock significantly reduced the level of EMC1 transcripts by 50% (RNAi-1) or 65% (RNAi-2). (**B**) Ubiquitous expression of *EMC1* RNAi by *Da-Gal4* or *Act-Gal4* causes lethality, as does glial-specific expression of *EMC1 RNAi* (*Repo > EMC1 RNAi-1* and *2*). Neuronal-specific expression of *EMC1 RNAi* by *Nsyb-Gal4* or *elav-Gal4* does not cause lethality. Co-expression of human *EMC1* reference rescued the lethality of *Repo > EMC1 RNAi-1* and *2* ($n = 9$ crosses/genotype). (**C**) Co-expression of human *EMC1* reference rescued the climbing defects of *Repo > EMC1 RNAi-1* and *2* flies. (**D**) Glial overexpression of wild-type fly *EMC1* is toxic, but expression of the variants is less toxic in flies. (**E**) Neuronal overexpression of either fly *EMC1* wild-type or variants does not cause lethality. Numbers indicate the ratio of o/e flies. Statistical analyses are one-way ANOVA followed by a Tukey's post hoc test. Results are mean ± s.e.m. ***$P < 0.001$.

Discussion

We describe three individuals with overlapping clinical features and de novo variants in *EMC1*, clustering within a few amino acids. EMC1, the largest EMC subunit, is a core subunit essential for the assembly and function of the EMC complex, and makes up part of its luminal domain (15,26). The dual functionality of the EMC complex, as a posttranslational insertase for TA proteins and a co-translational chaperone for membrane proteins, has been established in recent years (27,28). Other primary functions have been proposed for EMC, such as maintenance of rhodopsin homeostasis and photoreceptor function (20,29), which may stem from specific downstream functions of EMC (26). EMC1 harbors two recognizable domains: pyrroloquinoline quinone-like repeats (aa 21–252) within the region exposed to the ER lumen and a domain of unknown function (DUF1620, aa 787–992) in the transmembrane domain-containing C-terminus (30). However, the de novo variants described here do not affect either of these

and the clustering at amino acids 582–584, at the edge of a β-strand within a β-propeller, with proximity to the previously described de novo variant at 471, suggests that it will lead to mis-folded proteins or a third functional domain.

Drosophila melanogaster has been used as a powerful model organism to provide evidence of variant pathogenicity and study the mechanism of rare human genetic diseases (31,32). These include diseases caused by proteins associated with different organelles, such as mitochondria (33,34), peroxisomes (35,36), nuclei (37–39) and synaptic vesicles (40). Our studies indicate that both overexpression and knockdown of wild-type *EMC1* cause lethality in *Drosophila*. The imbalance of *EMC1* dosage compared with other subunits may lead to destabilization and degradation of the entire EMC complex (41). Interestingly, individuals with a heterozygous frameshift variant in *EMC1* (i.e. parents of an affected individual with a homozygous frameshift variant) remain healthy (7) and the probability of loss-of-function intolerance of the gene is 0 [observed/expected (o/e) ratio—0.79] (14). Thus, in humans, 50% of the gene dosage seems sufficient. Accordingly, the heterozygous missense variants studied here [p.(Pro582His), p.(Pro582Arg) and p.(Pro584His)] would be anticipated to potentially lead to disease via a dominant-negative effect, disrupting the function of the wild-type protein, or via a toxic gain-of-function. Nonetheless, in *Drosophila*, homologous mutations behave as loss-of-function variants, and this discrepancy remains to be resolved. A potential limitation of this work is that we did not assess the stability or steady-state level of the mutant proteins, which may affect protein function. Notably, sequencing of cDNA from an affected individual indicated that there were no mis-splicing events and that both alleles were present in fibroblasts. An intriguing possibility is that noncoding common variation may contribute to a further than expected tissue-specific decrease in EMC1 levels in affected individuals (42). However, this would not be expected to result from a common haplotype in the population because the four families are of varied ancestries.

Using cell-type-specific drivers in *Drosophila,* we were able to implicate glial dysfunction, rather than neuronal dysfunction, as the primary mechanism underlying EMC1-associated phenotypes. Glial function is critical for the maintenance of CNS homeostasis, and Drosophila has several glial subtypes, including perineurial glia, sub-perineurial glia, ensheathing glia, cortex glia and astrocyte-like glia (43,44). However, we could not find any significant lethality or climbing defects when we crossed *EMC1 RNAi*s with *mz97-Gal4* (ensheathing glia), *alrm-Gal4* (astrocyte-like glia), *NP2222-Gal4* (cortex glia) or *moody-Gal4* (perineurial glia) at Day 3 as observed with *Repo > EMC1 RNAi* (data not shown). Hence, it is not obvious which type of glia is/are susceptible to loss or gain of *EMC1,* which remains to be explored. Also, given that perineurial glia shares function with subperineurial glia (45), co-expression of *EMC1 RNAi* in both glia may show similar phenotypes as *Repo > EMC1 RNAi*.

Glial dysfunction has been implicated in a growing number of late-onset neurodegenerative diseases, including Alzheimer disease (46–48), amyotrophic lateral sclerosis and frontotemporal dementia (49) as well as in early onset Mendelian disorders, such as Rett syndrome (50), Mitchell syndrome (36), Alexander disease (51), X-linked adrenoleukodystrophy (52), metachromatic leukodystrophy (53) and Pelizaeus-Merzbacher disease (54). Moreover, genetic defects resulting in glial dysfunction have been shown to underlie cerebellar defects (55), similar to the phenotype seen in humans with *EMC1* variants. Although not yet explored in clinical practice, glial cell replacement has been suggested as a possible therapeutic strategy for neurological diseases (56).

Previous studies have shown that the EMC complex maintains ER homeostasis, and a deficiency of the EMC complex induces ER stress and an unfolded protein response (UPR) (57). UPR is initially protective to cells, but in situations of prolonged unresolved stress, the UPR can lead to apoptotic death of the stressed cell (58). Notably, ER stress and the UPR are closely associated with many myelin and myelinating glia disorders, including multiple sclerosis (59), Pelizaeus-Merzbacher disease (60), Vanishing White Matter Disease (60,61) and Charcot–Marie–Tooth disease (3,62,63). However, whether or not EMC1 variants (p.P582H, p. P582R and p. P584H) identified in human patients cause ER stress in glia, leading to neurologic phenotypes, needs to be explored.

In conclusion, our data further define the phenotypic spectrum associated with *EMC1* variants, provide proof of pathogenicity for *EMC1* variants within a defined domain and indicate that the primary defect in *EMC1*-associated disease is within glia rather than neurons.

Materials and Methods

Exome analysis

Following informed consent, exome sequencing and rare variant family based genomics were pursued on DNA extracted from whole blood of affected individuals from each unrelated sporadic proband, and from parents where available. Study design was trio exome sequencing in Families A and C, and duo in Family B, as the father was deceased. For Family A, exome sequencing was performed as previously described (64). In summary, capture of exons was done using an Agilent SureSelect Human All Exon 50 Mb kit (Santa Clara, CA). Sequencing was performed by BGI Copenhagen using Illumina HiSeq 4000 (San Diego, CA). Read mapping (BWA), calling (GATK) and annotation (in-house pipeline) were implemented at the Human Genetics Department of the Radboud University Medical Center. For Family B, capture of exons was done using an Agilent Clinical Research Exome kit (Santa Clara, CA). Targeted regions were sequenced on an Illumina HiSeq sequencing system (San Diego, CA) with 100 bp paired-end reads, to a

mean depth of coverage of 165X. Reads were aligned to reference genome GRCh37/UCSC hg19 and analysed for sequence variants using a custom-developed analysis tool. Additional sequencing technology and variant interpretation protocol have been previously described (65). For Family C, clinical exome sequencing was done at Ambry Genetics as previously described (66).

Fibroblast culture

Following informed consent, fibroblasts derived from a skin biopsy of Individual II-1 in Family A were cultured in flasks containing Dulbecco's Modified Eagle Medium, DMEM (gibco, LOT No. 2311544), 20% fetal bovine serum (Corning, LOT No. 35016116) and 1% Anti–Anti (gibco, LOT2176277) at 37°C with 5% CO_2.

RNA extraction and cDNA synthesis

RNA from fibroblast cell lines was isolated using the TRIzol® method and was further purified using the QIAGEN RNeasy® Mini Kit standard protocol (LOT No. 163035346). cDNA was then synthesized using the qScript™ cDNA SuperMix by Quanta BIOSCIENCES™ (Cat. No. 95048–025). The entire coding sequence of *EMC1* was amplified using QIAGEN HotStartTaq® *PLUS* DNA Polymerase, with the following primers: EMC1_cDNA_F1: 5′-CTGAGTGGGCTTCTCGTTTC-3′ and EMC1_cDNA_R1: 5′-TCTGCACTTCATTCCGACAG-3′; EMC1_cDNA_F2: 5′-ACTGCCCTAGTGAGCTTTGC-3′ and EMC1_cDNA_R2: 5′-TGCTCTGCATCCACCAAATA-3′; and EMC1_cDNA_F3: 5′-CACAGCTTTTCCAGCCACTC-3′ and EMC1_cDNA_R3: 5′-AGCTTCACCTGTGCCAGTCT-3′. Sequences were determined by Sanger sequencing.

3D modeling of protein structure

The molecular representations were produced with PyMOL Molecular Graphics System, Version 2.4.1, Schrödinger, LLC.

Drosophila strains and maintenance

EMC1^{655G} was a gift from Akiko Satoh (20) at Hiroshima University. The following stocks were obtained from the Bloomington Drosophila Stock Center (BDSC, Indiana University) and cultured at 25°C unless otherwise noted: y^1 *w∗; P {Act5C-GAL4} 25FO1/CyO,* y^+ (RRID: BDSC_441434), *w∗;da-GAL4* (RRID: BDSC_5460), w^{1118}*; P{GAL4}repo/TM3,Sb1* (RRID: BDSC_7415), *P{GAL4-elav.L}2/CyO* (RRID: BDSC_876535), y^1 *w∗; P{nSyb-GAL4.S}3* (RRID: BDSC_51635). The following stocks were obtained from the Vienna Drosophila Resource Center (VDRC): EMC1 RNAi-1: w^{1118}*; P{GD2851}v8477/TM3*, EMC1 RNAi-2: *P{KK102784}VIE-260B*.

Real-time polymerase chain reaction (PCR)

Flies were maintained at 18°C before eclosion. After eclosion, 1-day old adult male flies ($n = 20$) were used for heat shock treatment. First, flies were heat-shocked for 30 min at 37°C and kept at 29°C for 24 h. Next, flies were heat-shocked again for 30 min at 37°C and maintained at 29°C for 24 h. Then, flies were collected, and total RNA was extracted using TRIzol (Invitrogen, 15 596 026) following the manufacturer's instructions. cDNA synthesis and the removal of genomic DNA were carried out using All-In-One 5× RT MasterMix (abm, G592). Real-time PCR experiments were conducted in triplicates and analyzed using a CFX96TM Real-Time system (Bio-RAD) with iTaq Universal SYBR Green Supermix (Bio-rad, 1 725 121). Real-Time PCR steps were as follows; PCR reactions were initially incubated at 95°C for 3 min for polymerase activation and DNA denaturation. After the pre-treatment, reactions were subjected to the following thermal cycling conditions: 40 cycles of denaturation at 95°C for 5 s and annealing/extension at 60°C for 30 s. After cycling, the melting curve was analyzed to check the existence of nonspecific amplification. Experiments were repeated two times. All primers were synthesized (GENEWIZ) and purified with high-performance liquid chromatography (HPLC). Following primers with high primer efficiency (>95%) were used for amplification:

Rp49 F: TACAGGCCCAAGATCGTGAA (Tm:60).
Rp49 R: TCTCCTTGCGCTTCTTGGA (Tm:60).
Emc1 F: AAGGGCAAGGCCGGAGA (Tm:60).
Emc1 R: AGACGCATCTGTTCGTCGTT (Tm:60).

Immunohistochemistry of larva and adult CNS

For adult brains: adult flies were dissected and fixed in 4% PFA in PBS for 1 h at room temperature. Samples were then washed three times in PBS-Triton X-100 (0.2%) and permeabilizes in 0.2% PBST at room temperature. For third instar larvae, brains were dissected and fixed in 4% PFA in PBS at 4°C overnight and transferred to 0.2% Triton X-100 in PBS and washed three times for 10 min. All tissues were blocked in 5% normal goat serum with 0.2% Triton X-100 in PBS for 1 h at room temperature and incubated with primary antibodies: anti-Elav rat monoclonal: 1:200; anti-Repo mouse monoclonal: 1:50. Primary antibodies were incubated at 4°C overnight and then washed 3× with 0.2% Triton X-100 in PBS. Half of the samples were incubated with the secondary antibody conjugated to anti-mouse Alexa-647 or anti-rat Alexa-647. All secondaries were diluted 1:500 in 0.2% Triton X-100 in PBS and incubated at room temperature for 2 h, washed 4× and mounted in (mounting solution) and imaged with confocal microscopy (Leica Sp8X). Images were processed analyzed using Fiji (67).

Drosophila assays

The climbing assay was performed as described (36). In brief, we examined if negative geotaxis allows flies to reach the 7 cm mark on the vial. Flies were given a maximum of 30 s to reach this mark. For viability quantification, the total number of flies was assessed for each genotype, and correct genotypes were divided by the expected Mendelian ratio (38). Crosses were repeated a minimum of three times to obtain multiple biological replicates.

Generation of *EMC1 Drosophila* transgenics

UAS-EMC1 transgenics

Transgenic flies for *Drosophila UAS-EMC1* wildtype and variants (p.P506H, p.P506R and p.P509H) corresponding to equivalent amino acid changes observed in human subjects were generated as previously described (38). The entry EMC1 clone (GenBank: NM_001300286.1) was obtained from the Drosophila Genomics Resource Center (GEO03377, Cat. No. 1660079). Using Gateway cloning (Thermo Fisher Scientific), the EMC1 cDNA entry clone present in the pDONR223 vector was shuttled to the pGW-attB-HA (68). Site-directed mutagenesis was performed with the Q5 site-directed mutagenesis kit (NEB) followed by Sanger DNA sequencing for verification. The following forward and reverse primers were used to make *EMC1* variants: EMC1_p.P506H_F: 5′-AAACACTTTCATCTTCAGCCGTTGTGCACTATTTTGG-3′ and EMC1_p.P506H_R: 5′-GGCCGAGCGCTGGACAAT-3′; EMC1_p.P506R_F: 5′- AAACACTTTCGACTTCAGCCGTTG-TGC -3′ and EMC1_p.P506R_R: 5′- GGCCGAGCGCTGGA-CAAT −3′; and EMC1_p.P509H_F: 5′- CCACTTCAGCACT-TGTGCACTATTTTGGGC -3′ and EMC1_p.P509H_R: 5′- AAAGTGTTTGGCCGAGCG −3′.

Sanger verification of the ORFs was conducted with the following sequencing primers: EMC1_Rev1: CGAACTTTTTGATCTGGTCTTCGTAG; EMC1_Seq1: CGC-CATGTGGATCTACAGCA; EMC1_Seq2: CGACTGTAAGCA-GAAGCGCA; EMC1_Seq3: CGTCTGATTGTCCAGCGC; EMC1_Seq4: CGGTGCTGTACAAGTACATCAAC; EMC1_Seq5: CGACTCAGGGACGTGAAGAAG. All UAS-cDNA constructs were inserted into the VK37 (PBac{y[+]-attP}VK00037) docking site by ϕC31-mediated recombination (69).

EMC1 Kozak Gal4

The EMC1 KozakGAL4 allele is generated as described in literature (21,22). Briefly, the sgRNAs targeting 3′ and 5′ Untranslated Regions of EMC1 and 200 nt homology arms that flank the sgRNAcut sites are synthesized in pUC57_Kan_gw_OK2 vector. sgRNA sequences that target the EMC1 locus are (TAGTCGAAGGTCAGCAAGCAAGG) for 5′UTR and (TACTGCGACCAAATACCACAAGG) for 3′UTR (PAM sites underlined). KozakGAL4-polyA-3XP3-EGFP-polyA cassette is subcloned in the resulting vector from pM37-KozakGAL4 vector. The resulting plasmid is injected in embryos of flies expressing Cas9 in their germline as described in Lee *et al.* (70).

Ethics approval and consent to participate

Families A and B provided consent according to the Baylor-Hopkins Center for Mendelian Genomics (BHCMG) research protocol (H-29697). Family C was consented for exome sequencing in a clinical laboratory and submitted for publication in accordance with COMIRB (Colorado Multi-institution IRB) protocol no. 19–0172 (secondary use of clinical data and minimal risk).

Supplementary Material

Supplementary Material is available at *HMG* online.

Acknowledgements

The authors thank the families for their participation in this study.

Conflict of Interest statement. J.R.L. has stock ownership in 23andMe, is a paid consultant for Regeneron Genetics Center and is a co-inventor on multiple United States and European patents related to molecular diagnostics for inherited neuropathies, eye diseases and bacterial genomic fingerprinting. The Department of Molecular and Human Genetics at Baylor College of Medicine receives revenue from clinical genetic testing conducted at Baylor Genetics (BG) Laboratories. J.R.L serves on the Scientific Advisory Board of BG.

Funding

NIH grant U01 HG007703 and National Human Genome Research Institute (NHGRI) and National Heart Lung and Blood Institute (NHBLI) to the Baylor-Hopkins Center for Mendelian Genomics (BHCMG, UM1 HG006542, J.R.L.) and the U.S. National Institute of Neurological Disorders and Stroke (NINDS, R35NS105078, J.R.L.). H.C. is supported by the Warren Alpert Foundation. P.C.M. is supported by CIHR (MFE-164712). H.J.B. is supported by the Huffington Foundation, and the Jan and Dan Duncan Neurological Research Institute at Texas Children's Hospital. H.J.B. and H.C. research was also supported by the Eunice Kennedy Shriver National Institute of Child Health & Human Development of the National Institutes of Health (NIH) under award number P50HD103555 for the use of the Neurovisualization core facilities. The content is solely the responsibility of the authors and does not necessarily represent the official views of the NIH. Further support came from The Office of Research Infrastructure Programs of the NIH under the award numbers R24 OD022005 and R24 OD031447 to H.J.B. H.J.B. thanks HHMI for previous support.

References

1. Christianson, J.C., Olzmann, J.A., Shaler, T.A., Sowa, M.E., Bennett, E.J., Richter, C.M., Tyler, R.E., Greenblatt, E.J., Harper, J.W. and Kopito, R.R. (2011) Defining human ERAD networks through an integrative mapping strategy. *Nat. Cell Biol.*, **14**, 93–105.
2. Jonikas, M.C., Collins, S.R., Denic, V., Oh, E., Quan, E.M., Schmid, V., Weibezahn, J., Schwappach, B., Walter, P., Weissman, J.S. *et al.* (2009) Comprehensive characterization of genes required for protein folding in the endoplasmic reticulum. *Science*, **323**, 1693–1697.
3. Bai, L., You, Q., Feng, X., Kovach, A. and Li, H. (2020) Structure of the ER membrane complex, a transmembrane-domain insertase. *Nature*, **584**, 475–478.

4. Lahiri, S., Chao, J.T., Tavassoli, S., Wong, A.K., Choudhary, V., Young, B.P., Loewen, C.J. and Prinz, W.A. (2014) A conserved endoplasmic reticulum membrane protein complex (EMC) facilitates phospholipid transfer from the ER to mitochondria. *PLoS Biol.*, **12**, e1001969.
5. Abu-Safieh, L., Alrashed, M., Anazi, S., Alkuraya, H., Khan, A.O., Al-Owain, M., Al-Zahrani, J., Al-Abdi, L., Hashem, M., Al-Tarimi, S. *et al.* (2013) Autozygome-guided exome sequencing in retinal dystrophy patients reveals pathogenetic mutations and novel candidate disease genes. *Genome Res.*, **23**, 236–247.
6. Homsy, J., Zaidi, S., Shen, Y., Ware, J.S., Samocha, K.E., Karczewski, K.J., DePalma, S.R., McKean, D., Wakimoto, H., Gorham, J. *et al.* (2015) De novo mutations in congenital heart disease with neurodevelopmental and other congenital anomalies. *Science*, **350**, 1262–1266.
7. Harel, T., Yesil, G., Bayram, Y., Coban-Akdemir, Z., Charng, W.L., Karaca, E., Al Asmari, A., Eldomery, M.K., Hunter, J.V., Jhangiani, S.N. *et al.* (2016) Monoallelic and Biallelic variants in EMC1 identified in individuals with global developmental delay, Hypotonia, scoliosis, and cerebellar atrophy. *Am. J. Hum. Genet.*, **98**, 562–570.
8. Jin, S.C., Homsy, J., Zaidi, S., Lu, Q., Morton, S., DePalma, S.R., Zeng, X., Qi, H., Chang, W., Sierant, M.C. *et al.* (2017) Contribution of rare inherited and de novo variants in 2,871 congenital heart disease probands. *Nat. Genet.*, **49**, 1593–1601.
9. Geetha, T.S., Lingappa, L., Jain, A.R., Govindan, H., Mandloi, N., Murugan, S., Gupta, R. and Vedam, R. (2018) A novel splice variant in EMC1 is associated with cerebellar atrophy, visual impairment, psychomotor retardation with epilepsy. *Mol. Genet. Genomic. Med.*, **6**, 282–287.
10. Cabet, S., Lesca, G., Labalme, A., Des Portes, V., Guibaud, L., Sanlaville, D. and Pons, L. (2020) Novel truncating and missense variants extending the spectrum of EMC1-related phenotypes, causing autism spectrum disorder, severe global development delay and visual impairment. *Eur. J. Med. Genet.*, **63**, 103897.
11. Marquez, J., Criscione, J., Charney, R.M., Prasad, M.S., Hwang, W.Y., Mis, E.K., Garcia-Castro, M.I. and Khokha, M.K. (2020) Disrupted ER membrane protein complex-mediated topogenesis drives congenital neural crest defects. *J. Clin. Invest.*, **130**, 813–826.
12. Umair, M., Ballow, M., Asiri, A., Alyafee, Y., Al Tuwaijri, A., Alhamoudi, K.M., Aloraini, T., Abdelhakim, M., Althagafi, A.T., Kafkas, S. *et al.* (2020) EMC10 homozygous variant identified in a family with global developmental delay, mild intellectual disability, and speech delay. *Clin. Genet.*, **98**, 555–561.
13. Shao, D.D., Straussberg, R., Ahmed, H., Khan, A., Tian, S., Hill, R.S., Smith, R.S., Majmundar, A.J., Ameziane, N., Neil, J.E. *et al.* (2021) A recurrent, homozygous EMC10 frameshift variant is associated with a syndrome of developmental delay with variable seizures and dysmorphic features. *Genet. Med.*, **23**, 1158–1162.
14. Karczewski, K.J., Francioli, L.C., Tiao, G., Cummings, B.B., Alfoldi, J., Wang, Q., Collins, R.L., Laricchia, K.M., Ganna, A., Birnbaum, D.P. *et al.* (2020) The mutational constraint spectrum quantified from variation in 141,456 humans. *Nature*, **581**, 434–443.
15. Miller-Vedam, L.E., Brauning, B., Popova, K.D., Schirle Oakdale, N.T., Bonnar, J.L., Prabu, J.R., Boydston, E.A., Sevillano, N., Shurtleff, M.J., Stroud, R.M. *et al.* (2020) Structural and mechanistic basis of the EMC-dependent biogenesis of distinct transmembrane clients. *elife*, **9**, e62611.
16. Richardson, J.S. and Richardson, D.C. (2002) Natural beta-sheet proteins use negative design to avoid edge-to-edge aggregation. *Proc. Natl. Acad. Sci. U. S. A.*, **99**, 2754–2759.
17. Wang, J., Al-Ouran, R., Hu, Y., Kim, S.Y., Wan, Y.W., Wangler, M.F., Yamamoto, S., Chao, H.T., Comjean, A., Mohr, S.E. *et al.* (2017) MARRVEL: integration of human and model organism genetic resources to facilitate functional annotation of the human genome. *Am. J. Hum. Genet.*, **100**, 843–853.
18. Hu, Y., Flockhart, I., Vinayagam, A., Bergwitz, C., Berger, B., Perrimon, N. and Mohr, S.E. (2011) An integrative approach to ortholog prediction for disease-focused and other functional studies. *BMC Bioinformatics*, **12**, 357.
19. Sievers, F., Wilm, A., Dineen, D., Gibson, T.J., Karplus, K., Li, W., Lopez, R., McWilliam, H., Remmert, M., Soding, J. *et al.* (2011) Fast, scalable generation of high-quality protein multiple sequence alignments using Clustal Omega. *Mol. Syst. Biol.*, **7**, 539.
20. Satoh, T., Ohba, A., Liu, Z., Inagaki, T. and Satoh, A.K. (2015) dPob/EMC is essential for biosynthesis of rhodopsin and other multi-pass membrane proteins in drosophila photoreceptors. *eLife*, **4**, e06306.
21. Kanca, O., Zirin, J., Hu, Y., Tepe, B., Dutta, D., Lin, W.-W., Ma, L., Ge, M., Zuo, Z., Liu, L.-P. *et al.* (2021) An expanded toolkit for drosophila gene tagging using synthesized homology donor constructs for CRISPR mediated homologous recombination. https://doi.org/10.1101/2021.12.24.474112.
22. Kanca, O., Zirin, J., Garcia-Marques, J., Knight, S.M., Yang-Zhou, D., Amador, G., Chung, H., Zuo, Z., Ma, L., He, Y. *et al.* (2019) An efficient CRISPR-based strategy to insert small and large fragments of DNA using short homology arms. *Elife*, **8**, e51539.
23. Halfon, M.S., Kose, H., Chiba, A. and Keshishian, H. (1997) Targeted gene expression without a tissue-specific promoter: creating mosaic embryos using laser-induced single-cell heat shock. *Proc. Natl. Acad. Sci. U. S. A.*, **94**, 6255–6260.
24. Zhang, Y., Sloan, S.A., Clarke, L.E., Caneda, C., Plaza, C.A., Blumenthal, P.D., Vogel, H., Steinberg, G.K., Edwards, M.S., Li, G. *et al.* (2016) Purification and characterization of progenitor and mature human astrocytes reveals transcriptional and functional differences with mouse. *Neuron*, **89**, 37–53.
25. Davie, K., Janssens, J., Koldere, D., De Waegeneer, M., Pech, U., Kreft, L., Aibar, S., Makhzami, S., Christiaens, V., Bravo Gonzalez-Blas, C. *et al.* (2018) A single-cell transcriptome atlas of the aging drosophila brain. *Cell*, **174**, 982–998 e920.
26. Volkmar, N. and Christianson, J.C. (2020) Squaring the EMC - how promoting membrane protein biogenesis impacts cellular functions and organismal homeostasis. *J. Cell Sci.*, **133**, jcs234519.
27. Guna, A., Volkmar, N., Christianson, J.C. and Hegde, R.S. (2018) The ER membrane protein complex is a transmembrane domain insertase. *Science*, **359**, 470–473.
28. Shurtleff, M.J., Itzhak, D.N., Hussmann, J.A., Schirle Oakdale, N.T., Costa, E.A., Jonikas, M., Weibezahn, J., Popova, K.D., Jan, C.H., Sinitcyn, P. *et al.* (2018) The ER membrane protein complex interacts cotranslationally to enable biogenesis of multipass membrane proteins. *Elife*, **7**, e37018.
29. Xiong, L., Zhang, L., Yang, Y., Li, N., Lai, W., Wang, F., Zhu, X. and Wang, T. (2020) ER complex proteins are required for rhodopsin biosynthesis and photoreceptor survival in drosophila and mice. *Cell Death Differ.*, **27**, 646–661.
30. Ninagawa, S., Okada, T., Sumitomo, Y., Horimoto, S., Sugimoto, T., Ishikawa, T., Takeda, S., Yamamoto, T., Suzuki, T., Kamiya, Y. *et al.* (2015) Forcible destruction of severely misfolded mammalian glycoproteins by the non-glycoprotein ERAD pathway. *J. Cell Biol.*, **211**, 775–784.
31. Bellen, H.J., Wangler, M.F. and Yamamoto, S. (2019) The fruit fly at the interface of diagnosis and pathogenic mechanisms of rare and common human diseases. *Hum. Mol. Genet.*, **28**, R207–R214.
32. Baldridge, D., Wangler, M.F., Bowman, A.N., Yamamoto, S., Undiagnosed Diseases, N., Schedl, T., Pak, S.C., Postlethwait, J.H., Shin, J., Solnica-Krezel, L. *et al.* (2021) Model organisms contribute to

diagnosis and discovery in the undiagnosed diseases network: current state and a future vision. *Orphanet J. Rare Dis.*, **16**, 206.
33. Yoon, W.H., Sandoval, H., Nagarkar-Jaiswal, S., Jaiswal, M., Yamamoto, S., Haelterman, N.A., Putluri, N., Putluri, V., Sreekumar, A., Tos, T. *et al.* (2017) Loss of Nardilysin, a mitochondrial co-chaperone for alpha-Ketoglutarate dehydrogenase, promotes mTORC1 activation and neurodegeneration. *Neuron*, **93**, 115–131.
34. Harel, T., Yoon, W.H., Garone, C., Gu, S., Coban-Akdemir, Z., Eldomery, M.K., Posey, J.E., Jhangiani, S.N., Rosenfeld, J.A., Cho, M.T. *et al.* (2016) Recurrent De novo and Biallelic variation of ATAD3A, encoding a mitochondrial membrane protein, results in distinct neurological syndromes. *Am. J. Hum. Genet.*, **99**, 831–845.
35. Wangler, M.F., Chao, Y.H., Bayat, V., Giagtzoglou, N., Shinde, A.B., Putluri, N., Coarfa, C., Donti, T., Graham, B.H., Faust, J.E. *et al.* (2017) Peroxisomal biogenesis is genetically and biochemically linked to carbohydrate metabolism in drosophila and mouse. *PLoS Genet.*, **13**, e1006825.
36. Chung, H.L., Wangler, M.F., Marcogliese, P.C., Jo, J., Ravenscroft, T.A., Zuo, Z., Duraine, L., Sadeghzadeh, S., Li-Kroeger, D., Schmidt, R.E. *et al.* (2020) Loss- or gain-of-function mutations in ACOX1 cause axonal loss via different mechanisms. *Neuron*, **106**, 589–606 e586.
37. Chao, H.T., Davids, M., Burke, E., Pappas, J.G., Rosenfeld, J.A., McCarty, A.J., Davis, T., Wolfe, L., Toro, C., Tifft, C. *et al.* (2017) A syndromic neurodevelopmental disorder caused by De novo variants in EBF3. *Am. J. Hum. Genet.*, **100**, 128–137.
38. Marcogliese, P.C., Shashi, V., Spillmann, R.C., Stong, N., Rosenfeld, J.A., Koenig, M.K., Martinez-Agosto, J.A., Herzog, M., Chen, A.H., Dickson, P.I. *et al.* (2018) IRF2BPL is associated with neurological phenotypes. *Am. J. Hum. Genet.*, **103**, 245–260.
39. Chung, H.L., Mao, X., Wang, H., Park, Y.J., Marcogliese, P.C., Rosenfeld, J.A., Burrage, L.C., Liu, P., Murdock, D.R., Yamamoto, S. *et al.* (2020) De novo variants in CDK19 are associated with a syndrome involving intellectual disability and epileptic encephalopathy. *Am. J. Hum. Genet.*, **106**, 717–725.
40. Ansar, M., Chung, H.L., Al-Otaibi, A., Elagabani, M.N., Ravenscroft, T.A., Paracha, S.A., Scholz, R., Abdel Magid, T., Sarwar, M.T., Shah, S.F. *et al.* (2019) Bi-allelic variants in IQSEC1 cause intellectual disability, developmental delay, and short stature. *Am. J. Hum. Genet.*, **105**, 907–920.
41. Pleiner, T., Hazu, M., Tomaleri, G.P., Januszyk, K., Oania, R.S., Sweredoski, M.J., Moradian, A., Guna, A. and Voorhees, R.M. (2021) WNK1 is an assembly factor for the human ER membrane protein complex. *Mol. Cell*, **81**, 2963–2704.
42. Wu, N., Ming, X., Xiao, J., Wu, Z., Chen, X., Shinawi, M., Shen, Y., Yu, G., Liu, J., Xie, H. *et al.* (2015) TBX6 null variants and a common hypomorphic allele in congenital scoliosis. *N. Engl. J. Med.*, **372**, 341–350.
43. Yildirim, K., Petri, J., Kottmeier, R. and Klambt, C. (2019) Drosophila glia: few cell types and many conserved functions. *Glia*, **67**, 5–26.
44. Freeman, M.R. (2015) Drosophila central nervous system glia. *Cold Spring Harb. Perspect. Biol.*, **7**, a020552.
45. Winkler, B., Funke, D., Benmimoun, B., Speder, P., Rey, S., Logan, M.A. and Klambt, C. (2021) Brain inflammation triggers macrophage invasion across the blood-brain barrier in drosophila during pupal stages. *Sci. Adv.*, **7**, eabh0050.
46. Liu, L., Zhang, K., Sandoval, H., Yamamoto, S., Jaiswal, M., Sanz, E., Li, Z., Hui, J., Graham, B.H., Quintana, A. *et al.* (2015) Glial lipid droplets and ROS induced by mitochondrial defects promote neurodegeneration. *Cell*, **160**, 177–190.
47. Liu, L., MacKenzie, K.R., Putluri, N., Maletic-Savatic, M. and Bellen, H.J. (2017) The glia-neuron lactate shuttle and elevated ROS promote lipid synthesis in neurons and lipid droplet accumulation in glia via APOE/D. *Cell Metab.*, **26**, 719–737 e716.
48. Guo, T., Zhang, D., Zeng, Y., Huang, T.Y., Xu, H. and Zhao, Y. (2020) Molecular and cellular mechanisms underlying the pathogenesis of Alzheimer's disease. *Mol. Neurodegener.*, **15**, 40.
49. Ghasemi, M., Keyhanian, K. and Douthwright, C. (2021) Glial cell dysfunction in C9orf72-related amyotrophic lateral sclerosis and frontotemporal dementia. *Cell*, **10**, 249.
50. Jin, X.R., Chen, X.S. and Xiao, L. (2017) MeCP2 deficiency in neuroglia: new progress in the pathogenesis of Rett syndrome. *Front. Mol. Neurosci.*, **10**, 316.
51. Brenner, M., Johnson, A.B., Boespflug-Tanguy, O., Rodriguez, D., Goldman, J.E. and Messing, A. (2001) Mutations in GFAP, encoding glial fibrillary acidic protein, are associated with Alexander disease. *Nat. Genet.*, **27**, 117–120.
52. Manor, J., Chung, H., Bhagwat, P.K. and Wangler, M.F. (2021) ABCD1 and X-linked adrenoleukodystrophy: a disease with a markedly variable phenotype showing conserved neurobiology in animal models. *J. Neurosci. Res.*, **99**, 3170–3181.
53. Bergner, C.G., van der Meer, F., Winkler, A., Wrzos, C., Turkmen, M., Valizada, E., Fitzner, D., Hametner, S., Hartmann, C., Pfeifenbring, S. *et al.* (2019) Microglia damage precedes major myelin breakdown in X-linked adrenoleukodystrophy and metachromatic leukodystrophy. *Glia*, **67**, 1196–1209.
54. Saher, G., Rudolphi, F., Corthals, K., Ruhwedel, T., Schmidt, K.F., Lowel, S., Dibaj, P., Barrette, B., Mobius, W. and Nave, K.A. (2012) Therapy of Pelizaeus-Merzbacher disease in mice by feeding a cholesterol-enriched diet. *Nat. Med.*, **18**, 1130–1135.
55. Basson, M.A. and Wingate, R.J. (2013) Congenital hypoplasia of the cerebellum: developmental causes and behavioral consequences. *Front. Neuroanat.*, **7**, 29.
56. Almad, A.A. and Maragakis, N.J. (2012) Glia: an emerging target for neurological disease therapy. *Stem Cell Res Ther*, **3**, 37.
57. Richard, M., Boulin, T., Robert, V.J., Richmond, J.E. and Bessereau, J.L. (2013) Biosynthesis of ionotropic acetylcholine receptors requires the evolutionarily conserved ER membrane complex. *Proc. Natl. Acad. Sci. U. S. A.*, **110**, E1055–E1063.
58. Sano, R. and Reed, J.C. (2013) ER stress-induced cell death mechanisms. *Biochim. Biophys. Acta*, **1833**, 3460–3470.
59. Cunnea, P., Mhaille, A.N., McQuaid, S., Farrell, M., McMahon, J. and FitzGerald, U. (2011) Expression profiles of endoplasmic reticulum stress-related molecules in demyelinating lesions and multiple sclerosis. *Mult. Scler.*, **17**, 808–818.
60. Southwood, C.M., Garbern, J., Jiang, W. and Gow, A. (2002) The unfolded protein response modulates disease severity in Pelizaeus-Merzbacher disease. *Neuron*, **36**, 585–596.
61. van Kollenburg, B., van Dijk, J., Garbern, J., Thomas, A.A., Scheper, G.C., Powers, J.M. and van der Knaap, M.S. (2006) Glia-specific activation of all pathways of the unfolded protein response in vanishing white matter disease. *J. Neuropathol. Exp. Neurol.*, **65**, 707–715.
62. Khajavi, M. and Lupski, J.R. (2008) Balancing between adaptive and maladaptive cellular stress responses in peripheral neuropathy. *Neuron*, **57**, 329–330.
63. Khajavi, M., Shiga, K., Wiszniewski, W., He, F., Shaw, C.A., Yan, J., Wensel, T.G., Snipes, G.J. and Lupski, J.R. (2007) Oral curcumin mitigates the clinical and neuropathologic phenotype of the trembler-J mouse: a potential therapy for inherited neuropathy. *Am. J. Hum. Genet.*, **81**, 438–453.
64. Neveling, K., Feenstra, I., Gilissen, C., Hoefsloot, L.H., Kamsteeg, E.J., Mensenkamp, A.R., Rodenburg, R.J., Yntema, H.G.,

Spruijt, L., Vermeer, S. *et al.* (2013) A post-hoc comparison of the utility of sanger sequencing and exome sequencing for the diagnosis of heterogeneous diseases. *Hum. Mutat.*, **34**, 1721–1726.

65. Retterer, K., Juusola, J., Cho, M.T., Vitazka, P., Millan, F., Gibellini, F., Vertino-Bell, A., Smaoui, N., Neidich, J., Monaghan, K.G. *et al.* (2016) Clinical application of whole-exome sequencing across clinical indications. *Genet. Med.*, **18**, 696–704.
66. Farwell, K.D., Shahmirzadi, L., El-Khechen, D., Powis, Z., Chao, E.C., Tippin Davis, B., Baxter, R.M., Zeng, W., Mroske, C., Parra, M.C. *et al.* (2015) Enhanced utility of family-centered diagnostic exome sequencing with inheritance model-based analysis: results from 500 unselected families with undiagnosed genetic conditions. *Genet. Med.*, **17**, 578–586.
67. Schindelin, J., Arganda-Carreras, I., Frise, E., Kaynig, V., Longair, M., Pietzsch, T., Preibisch, S., Rueden, C., Saalfeld, S., Schmid, B. *et al.* (2012) Fiji: an open-source platform for biological-image analysis. *Nat. Methods*, **9**, 676–682.
68. Bischof, J., Bjorklund, M., Furger, E., Schertel, C., Taipale, J. and Basler, K. (2013) A versatile platform for creating a comprehensive UAS-ORFeome library in drosophila. *Development*, **140**, 2434–2442.
69. Venken, K.J., He, Y., Hoskins, R.A. and Bellen, H.J. (2006) P[acman]: a BAC transgenic platform for targeted insertion of large DNA fragments in D. melanogaster. *Science*, **314**, 1747–1751.
70. Lee, P.T., Zirin, J., Kanca, O., Lin, W.W., Schulze, K.L., Li-Kroeger, D., Tao, R., Devereaux, C., Hu, Y., Chung, V. *et al.* (2018) A gene-specific T2A-GAL4 library for drosophila. *elife*, **7**, e35574.